THE JOURNAL OF BIOLOGICAL CHEMISTRY VOL. 286, NO. 6, pp. 4589–4597, February 11, 2011

Fatty Acid (FFA) Transport in Cardiomyocytes Revealed by Imaging Unbound FFA Is Mediated by an FFA Pump Modulated by the CD36 Protein*

Received for publication, September 4, 2010, and in revised form, November 30, 2010 Published, JBC Papers in Press, December 8, 2010, DOI 10.1074/jbc.M110.182162

Andrew N. Carley[1] **and Alan M. Kleinfeld**[2]

From the Torrey Pines Institute for Molecular Studies, San Diego, California 92121

Free fatty acid (FFA) transport across the cardiomyocyte plasma membrane is essential to proper cardiac function, but the role of membrane proteins and FFA metabolism in FFA transport remains unclear. Metabolism is thought to maintain intracellular FFA at low levels, providing the driving force for FFA transport, but intracellular FFA levels have not been measured directly. We report the first measurements of the intracellular unbound FFA concentrations (FFA_i) in cardiomyocytes. The fluorescent indicator of FFA, ADIFAB (acrylodan-labeled rat intestinal fatty acid-binding protein), was microinjected into isolated cardiomyocytes from wild type (WT) and FAT/CD36 null C57B1/6 mice. Quantitative imaging of ADIFAB fluorescence revealed the time courses of FFA influx and efflux. For WT mice, rate constants for efflux ($\sim 0.02\ s^{-1}$) were twice influx, and steady state FFA_i were more than 3-fold larger than extracellular unbound FFA (FFA_o). The concentration gradient and the initial rate of FFA influx saturated with increasing FFA_o. Similar characteristics were observed for oleate, palmitate, and arachidonate. FAT/CD36 null cells revealed similar characteristics, except that efflux was 2–3-fold slower than WT cells. Rate constants determined with intracellular ADIFAB were confirmed by measurements of intracellular pH. FFA uptake by suspensions of cardiomyocytes determined by monitoring FFA_o using extracellular ADIFAB confirmed the influx rate constants determined from FFA_i measurements and demonstrated that rates of FFA transport and etomoxir-sensitive metabolism are regulated independently. We conclude that FFA influx in cardiac myocytes is mediated by a membrane pump whose transport rate constants may be modulated by FAT/CD36.

Regulation of FFA[3] transport across the cardiomyocyte membrane is essential for cardiovascular health and dysregulation may result in myocardial lipotoxicity (1). However, the mechanisms governing FFA transport across cell membranes are not well understood (2, 3). Proposed mechanisms include rapid flip-flop through the lipid phase of the plasma membrane (4) or a protein-mediated mechanism (2, 3, 5). Proteins reported to be correlated with FFA transport in cardiac or muscle cells include FAT/CD36, FABPpm, and FATP4 (6–10).

In previous studies of FFA transport we found virtually identical characteristics in adipocytes and preadipocytes, suggesting involvement of an unknown protein because FAT/CD36, FABPpm, and FATP4 are expressed poorly or not at all in preadipocytes (2, 11–13). Transport in these studies was observed by imaging the concentration of intracellular unbound FFA (FFA_i) (11, 12, 14). This allowed us to directly monitor the movement of unbound FFA (FFA_u) from the extracellular medium and into the cytosol.

Because FFA transport plays a vital role in the heart and because our adipocyte/preadipocyte results raise the possibility that novel FFA transport mechanisms might exist in other tissues, we have investigated FFA transport in cardiomyocytes isolated from wild type (WT) adult C57BL/6 mice and FAT/$CD36^{-/-}$ mice on the C57BL/6 background. We used several methods to monitor FFA transport in this study, so that key findings were confirmed independently of a specific method. These methods included 1) quantitative imaging of FFA_i using a sensor of FFA, ADIFAB (acrylodan-labeled rat intestinal fatty acid-binding protein), 2) using the pH indicator BCECF-AM (2′,7′-bis(2-carboxyethyl)-5-(and-6)-carboxyfluorescein, acetoxymethyl ester) to monitor FFA influx and efflux, and 3) a new method to determine FFA uptake by monitoring the extracellular unbound FFA concentration (FFA_o) using ADIFAB in the extracellular medium.

This study provides the first measurements of FFA_i in cardiac cells and the first direct measurements of FFA influx and efflux across the cardiac plasma membrane. The results suggest that FFAs are pumped into cardiomyocytes and that FAT/CD36 interacts with the transporter/pump so that it significantly modifies the rate of efflux and, to a lesser extent, the rate of influx. The results significantly alter current views of the mechanisms of FFA transport in cardiac myocytes and may provide insights for understanding the role of FFA in cardiac dysregulation.

EXPERIMENTAL PROCEDURES

Buffering the Extracellular Unbound FFA Concentration—Measurements of FFA transport were performed by clamping

* This work was supported, in whole or in part, by National Institutes of Health Grant DK058762 (NIDDK).

[1] Supported by a postdoctoral fellowship from the American Heart Association.

[2] To whom correspondence should be addressed: Torrey Pines Institute for Molecular Studies, 3550 General Atomics Court, San Diego, CA 92121. Tel.: 858-455-3724; Fax: 858-455-3792; E-mail: akleinfeld@tpims.org.

[3] The abbreviations used are: FFA, free fatty acid; FFA_u, unbound FFA; FFA_o, extracellular unbound FFA; FFA_i, intracellular unbound FFA; ADIFAB, acrylodan labeled rat intestinal fatty acid-binding protein; BCECF-AM, 2′,7′-bis(2-carboxyethyl)-5-(and-6)-carboxyfluorescein, acetoxymethyl ester; k_{in}, influx rate constant; k_{out}, efflux rate constant; K_p, partition coefficient; OA, oleate; OA_i, intracellular unbound OA; OA_o, extracellular unbound OA; pH_i, intracellular pH.

FFA_o at fixed values using complexes of FFA and BSA as described previously (11). Complexes of FFA-BSA were prepared by mixing aliquots of sodium salts (Nu-Chek Prep) of the FFA from a 50 mM stock solution of the FFA in water plus 4 mM NaOH at 37 °C with a 300–900 μM BSA (Sigma) solution in Na-HEPES (20 mM HEPES, 140 mM NaCl, 5.5 mM glucose, 5 mM KCl, 1 mM NaH_2PO_4, and 1 mM $MgSO_4$ at pH 7.4) also at 37 °C except for palmitate, which was prepared with its stock alkaline solution raised to 70 °C. Unless otherwise stated "BSA" indicates fatty acid-free BSA (fraction V, Sigma) and was prepared as a solution in Na-HEPES. BSA concentrations were determined by measuring absorption at 280 nm. For experiments in which cells underwent metabolic inhibition with oligomycin and 2-deoxyglucose, glucose was omitted from Na-HEPES. The FFA_u for each complex was determined using ADIFAB (FFA Sciences, San Diego) as described previously (14, 15). Measuring FFA_u directly is critical for correctly interpreting transport results especially at high FFA_o where saturation of cellular FFA transport is most apparent and where buffering of FFA_o by BSA is weakest. Under weak buffering conditions the actual FFA_o may be smaller than calculated using BSA binding constants, thereby giving the appearance of saturation.

Cardiac Myocyte Isolation—C57BL/6 mice (male, 8–25 weeks of age) were obtained from Jackson Laboratories (San Diego, CA). FAT/CD36$^{-/-}$ mice (male, 8–25 weeks of age) maintained on the C57BL/6 background and associated control mice were gifts from Dr. Nada Abumrad (Washington University in St. Louis). Mice had *ad libitum* access to food and water and were maintained on a 12-h light:12-h dark cycle. Cardiac myocytes were isolated from adult mice by collagenase perfusion as described previously (16). Briefly, mice were injected intraperitoneally with 100 units of heparin 20 min before administration of sodium pentobarbital (250 mg/kg intraperitoneally). The heart was arrested in ice-cold Buffer A containing 120 mM NaCl, 5.4 mM KCl, 1.2 mM $MgSO_4$, 1.2 mM NaH_2PO_4, 5.5 mM glucose, 20 mM $NaHCO_3$, 0.6 mM $CaCl_2$, 10 mM 2,3-butanedione monoxime, and 5 mM taurine, pH 7.5. The aorta was cannulated, and the heart underwent retrograde perfusion with Buffer A without calcium. The temperature of the perfusate was maintained at 37 °C and gassed with 95% O_2, 5% CO_2 before use. After 4 min, the buffer was changed to Buffer A plus 25 μM $CaCl_2$ and 59 units/ml type II collagenase (Worthington) for 15 min, and the coronary flow rate was set to 2.5 ml/min. The heart underwent further digestion (5–10 min) in a shaker bath (90 rpm) at 37 °C in Buffer A plus 50 μM $CaCl_2$, collagenase, and 1% BSA. Isolated cardiomyocytes were obtained from the digested tissue after gentle trituration and centrifugation for 1 min at 500 × *g*. The calcium concentration of the cardiomyocyte suspension was then increased in a stepwise fashion from 50 μM to 1 mM.

For measurements of FFA transport by microscopy, cells were plated on laminin-coated glass coverslips (20–25 μg/ml) in minimal essential medium (Sigma) plus 2.5% fetal bovine serum and 1% penicillin/streptomycin and allowed to attach for 1 h in an incubator (37 °C, 5% CO_2). The medium was then exchanged for minimal essential media plus 1% penicillin/streptomycin (serum-free). For FFA uptake experiments cells were maintained in suspension in Na-HEPES + 1 mM $CaCl_2$.

Fluorescence Microscopy and Microinjection—Fluorescence microscopy and microinjection of cells with ADIFAB were performed essentially as described previously (11) but with improved microscopy and modifications to permit successful microinjection in freshly isolated murine cardiac myocytes (17). A Nikon Eclipse TE2000-U inverted fluorescent microscope was used, primarily with a 40× S Fluor 40×/1.30 Oil DIC H/N2 objective, a Lumen 200 fluorescence illumination system, and a Photometrics Cascade II-512 EMCCD camera for detection. A Sutter Lambda 10-2 device was used to control the excitation shutter and the excitation and emission filters. Cells seeded on laminin-coated coverslips were placed in a perfusion chamber (Warner RC-26G) and heated using a Warner Instrument heating platform. Coverslips with attached cardiac myocytes were washed twice with Na-HEPES, and the buffer was then changed to Li-HEPES (20 mM HEPES, 140 mM LiCl, 5.5 mM glucose, 5 mM KCl, 1 mM NaH_2PO_4, and 1 mM $MgSO_4$ at pH 7.4). Cardiac myocytes were microinjected (Eppendorf) with ADIFAB (400–800 μM in glucose-free Li-HEPES). After microinjection, the coverslips were washed with Na-HEPES followed by a 5-min incubation in Na-HEPES plus 600 μM BSA followed by two additional washes in Na-HEPES.

FFA influx into the cells was initiated by exchanging Na-HEPES for a FFA-BSA complex at a defined FFA_o (600 μM BSA). Cells were excited at 380 nm, and images at 505 and 435 nm were collected at intervals of 10–20 s at the start of influx, at 30 s when cells were approaching steady state, and at 40–50 s at steady state. Before efflux was initiated, the perfusion chamber media was saved to determine FFA_o by fluorometry with ADIFAB (11). Efflux was initiated by exchanging the FFA-BSA complex for 600 μM BSA in the perfusion chamber. Images were collected at intervals of 10–20 s at the start of efflux, at 30 s upon approaching steady state, and at 40 s at steady state. At completion, the medium was removed, and the cells were washed twice with Na-HEPES before starting the next transport cycle. Typically 1–3 cycles were analyzed per coverslip with 1–5 cells per field. Image processing for evaluating the transport time course from changes in the ADIFAB ratio images (Fig. 1) was performed as described previously (11, 18). The rise in the ADIFAB ratio during influx and the decrease in the ADIFAB ratio during efflux were each fit to a single exponential decay from which we obtained the influx (k_{in}) and efflux (k_{out}) rate constants (in units of s^{-1}), respectively. Initial rates of influx and efflux were determined from the rate of change of FFA_i and are, therefore, presented in units of nM/s.

For BCECF-AM measurements the cells were first loaded with 2 μM BCECF-AM in Na-HEPES for 15 min before initiating transport measurements. Cells were then incubated with Na-HEPES + 600 μM BSA for 5 min and washed 7 times with Na-HEPES. BCECF-AM measurements were performed using a 20× Plan Apo 20×/0.75 DIC N2 objective, which allowed more cells to be monitored than with the 40× objec-

tive. Cells were excited at 440 and 485 nm, and emission was measured at 530 nm.

Oligomycin Plus 2-Deoxyglucose Treatment and Inhibition of FFA Oxidation—Cells attached to coverslips underwent metabolic inhibition with 10 μg/ml oligomycin (Sigma) and 37 mM 2-deoxyglucose (Sigma) in Na-HEPES without glucose for 30 min at 37 °C to deplete cellular ATP (11, 19, 20). Control experiments were performed by incubating cells in Na-HEPES with glucose for 30 min. In a previous study we microinjected ADIFAB in a group of cells, measured transport, added oligomycin and deoxyglucose, incubated for 60 min, and then re-measured transport on the same cells (11). We have since found that results were more consistent if cells were treated before microinjection, possibly because of a modification of ADIFAB during the 60-min incubation in the presence of oligomycin and deoxyglucose (12). In the present study we used different cells (on separate coverslips) to measure transport in ATP replete and in oligomycin-and deoxyglucose-treated cells. FFA oxidation was inhibited by incubating cardiac myocytes ($1–2 \times 10^5$ cells/ml) with 10 μM etomoxir (Sigma) for 15 min at 37 °C followed by washing with Na-HEPES + 1 mM $CaCl_2$.

Measuring FFA Uptake by Monitoring FFA_o—In the measurements for monitoring FFA_i, in which cells were microinjected with ADIFAB, FFA_o was clamped by using FFA-BSA complexes with large BSA concentrations so that FFA_o did not change significantly during the FFA transport time course. However, if BSA concentration is reduced sufficiently, the amount of FFA that is transferred to the cells can be an appreciable fraction of the total extracellular FFA pool. For such weak buffering conditions, FFA_o may decrease significantly as FFA transfers from the extracellular FFA pool (BSA bound and unbound FFA) to the cells. The time course of this transfer of FFA to the cells, which represents FFA uptake without washing, can be measured by using ADIFAB in the extracellular medium to monitor FFA_o. Because the calibration of extracellular ADIFAB in defined media is well established (15), such measurements should provide a robust and independent test of FFA transport characteristics.

FFA transfer to suspensions of cardiac myocytes was measured using cuvette fluorometry. An aqueous solution of 1.5 ml containing 0.2 μM ADIFAB and an oleate-BSA complex in Na-HEPES plus 1 mM $CaCl_2$, in which the BSA concentration was 10 μM, was added to a 10×10-mm glass cuvette. The cuvette was placed in a magnetically stirred thermostated (37 °C) cuvette holder of a Fluorolog 3 fluorometer (J-Y Horiba). The ADIFAB fluorescence was excited at 386 nm, and emission intensities at 505 and 432 nm were acquired continuously every 8 s. Before monitoring FFA uptake, cells were incubated with 600 μM BSA plus 1 mM $CaCl_2$ for 5 min and then washed twice with Na-HEPES plus 1 mM $CaCl_2$. The cardiac myocytes were resuspended at $\sim 5 \times 10^4$ cells/50 μl. This volume of cells was added to the stirred ADIFAB plus oleate (OA)-BSA-containing cuvette. The ratio of ADIFAB 505 to 432 nm intensities was monitored continuously to determine OA_o, and thereby the time course of uptake was established.

The concentration of total FFA in the extracellular medium during uptake was estimated using the measured FFA_o and the parameters for FFA binding to BSA measured previously (21) from which we found,

$$[A_b]/[A_t] = M[\mathrm{FFA}_u]/(K_d + [\mathrm{FFA}_u]) \quad \text{(Eq. 1)}$$

where $[A_b]$ = concentration of BSA bound FFA, $[A_t]$ = total concentration of BSA (protein), M = number of FFA binding sites per BSA, K_d = dissociation constant for FFA, and $[FFA_u]$ is the unbound concentration in equilibrium with BSA. Because total FFA $\gg FFA_u$, total FFA $\approx A_b$. For OA, $M = 7$ and at 37 °C, $K_d = 14$ nM (22). The total OA was, therefore, calculated as

$$[\mathrm{OA}] = 7[\mathrm{BSA}][\mathrm{OA}_o]/(14 + [\mathrm{OA}_o]) \quad \text{(Eq. 2)}$$

Estimation of FFA_i from Total Intracellular FFA and Total Intracellular Lipid—FFA_i was estimated from the concentration of total FFA transferred to the cells, as determined by uptake (Equation 2) and the concentration of total intracellular lipid, as determined by Forsdahl and Larsen (23). The estimate assumes, as in Ref, 24, that FFA_i is in equilibrium with total cellular FFA, which leads to,

$$[\mathrm{FFA}_i] = [\mathrm{FFA}]/(1 + 0.8K_p[L]) \quad \text{(Eq. 3)}$$

where 0.8 is the volume (in liters) per mol of lipid (25), K_p is the FFA/lipid partition coefficient, which for OA (26) is 4×10^5, and $[L]$ is the molar lipid concentration.

Statistical Analysis—Tabulated results are presented as the mean ± S.E. Sample means were compared by *t* test. A runs test (Prism 5, GraphPad software) was used to determine whether the initial rate of influx *versus* OA_o deviated significantly ($p < 0.05$) from linearity.

RESULTS

FFA Transport in WT Cardiomyocytes Microinjected with ADIFAB—FFA influx and efflux was monitored in cardiomyocytes that retained their rod-shaped morphology after microinjection with ADIFAB (Fig. 1*A*, *panel 1*). Transport of FFA, in this case OA, was reflected in the change of the false color fluorescence ratio images as intracellular ADIFAB responded to the change in the concentration of intracellular unbound oleate OA_i (Fig. 1*A*). Quantification of a series of such images was used to generate the OA transport time course (Fig. 1*B*). Influx was manifested by the increase in OA_i from base line to steady state in ~300 s followed by efflux as OA_i returned to base line after the concentration of extracellular unbound oleate (OA_o) was reduced to zero. Influx rate constants (k_{in}) were approximately half the efflux rate constants (k_{out}). Moreover, once OA_i reached steady state, OA_i became substantially larger than OA_o, and this $OA_i > OA_o$ gradient was maintained until efflux was initiated. Similar transport characteristics were found for palmitate and arachidonate (Table 1).

FFA Transport Monitored Using BCECF-AM—Translocation of FFA between the outside and inside surfaces of membranes alters intracellular pH (pH_i). BCECF-AM, the fluorescence pH_i indicator, was used to monitor FFA membrane

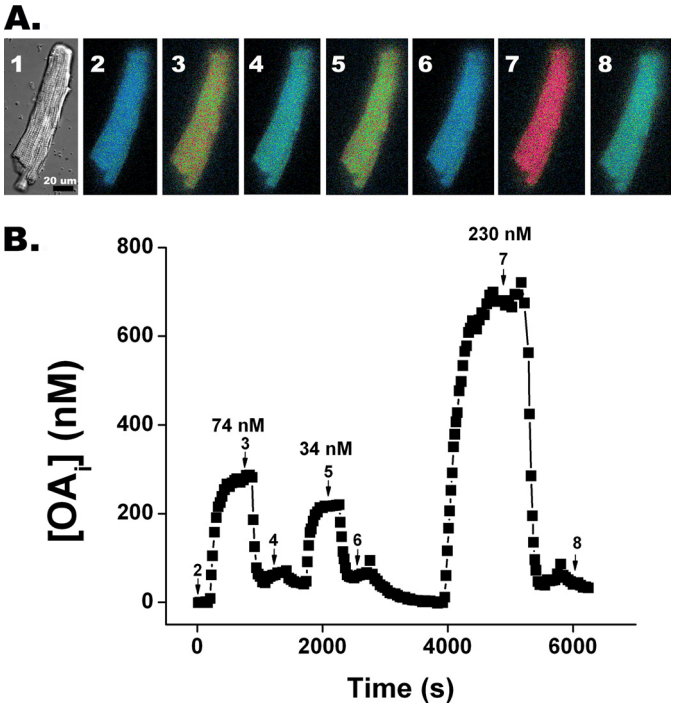

FIGURE 1. **FFA transport in a cardiomyocyte monitored by quantitative imaging of intracellular unbound oleate.** *A*, differential interference contrast and ratio fluorescence images of a cardiomyocyte microinjected with ADIFAB at different times after changing OA_o is shown. *Panel 1* is a differential contrast image of a typical cardiomyocyte after ADIFAB microinjection. *Panels 2–8* are ADIFAB fluorescence ratio (505/432 nm) images represented in "false color" in which *blue* corresponds to low and *red* to high OA_i, acquired at select times during three transport cycles (*numbered arrows* indicate where during the time course shown in *B* the images were acquired). *Panel 2* represents OA_i at time 0 when $OA_o = 0$. At 100 s OA_o was increased to 74 nM, and *panel 3* is at steady state after ~350 s. After ~1000 s the media was replaced so that OA_o was clamped at 0 nM and OA_i returned to base line (*panel 4*). *Panels 5–8* represent the corresponding images for cycles 2 and 3. *B*, quantitation of complete time courses for the three cycles were determined by whole cell averaging of OA_i. OA_o for each cycle is indicated *above* the steady state levels.

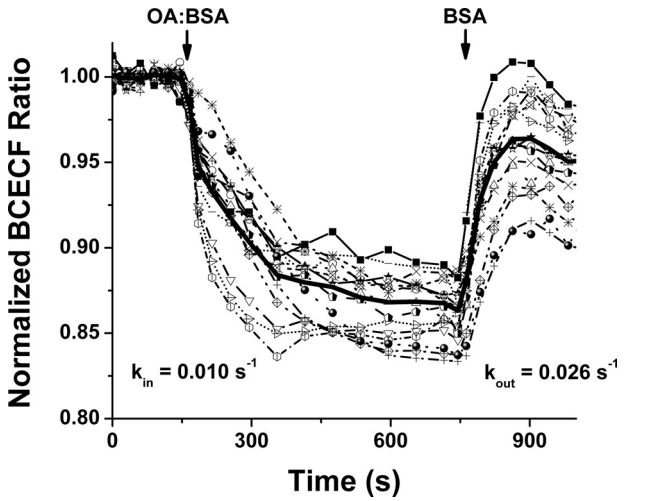

FIGURE 2. **Oleate transport cycle measured in BCECF-AM-loaded WT cardiomyocytes.** Oleate transport was measured by the change in pH_i as determined from the fluorescence responses in 18 BCECF-AM-loaded cardiomyocytes. Time courses are shown for individual cells and the average of all cells (*bold line*). Cells were initially clamped at $OA_o = 0$ nM. At ~200 s an OA-BSA complex was added with $OA_o = 250$ nM, leading to a decrease in pH_i that decayed with $k_{in} = 0.0096\ s^{-1}$. At ~750 s OA_o was again clamped to 0, resulting in a increase in pH_i with $k_{out} = 0.026\ s^{-1}$.

TABLE 1

FFA transport parameters measured in WT cardiomyocytes

Numbers of transport cycles are indicated in parentheses. Results were obtained using hearts from 14, 5, and 2 C57BL/6 mice for OA, arachidoniate, and palmitate, respectively.

FFA	k_{in}	k_{out}	FFA_i/FFA_o
	s^{-1}	s^{-1}	
OA	0.0096 ± 0.0003 (154)	0.020 ± 0.001 (115)	3.4 ± 0.1 (154)
Arachidonate	0.0104 ± 0.0007 (81)	0.021 ± 0.002 (33)	3.9 ± 0.1 (81)
Palmitate	0.013 ± 0.001 (29)	0.025 ± 0.002 (29)	4.2 ± 0.3 (30)

translocation in BCECF-AM-loaded cardiomyocytes (Fig. 2) as described previously for cardiomyocytes and adipocytes (11, 27, 34). Transport rate constants, ($k_{in} = 0.0096 \pm 0.0009\ s^{-1}$) and ($k_{out} = 0.026 \pm 0.005\ s^{-1}$), obtained from measurements of pH_i, were indistinguishable from those obtained from OA_i time courses in ADIFAB-loaded cells (Table 1). The equivalence of rate constants from intracellular measurements of pH_i and FFA_i supports the use of intracellular ADIFAB as an accurate indicator of FFA kinetics.

FFA Uptake—Intracellular ADIFAB might be affected by unknown factors in the intracellular environment, and measurements of single cells might not reflect accurately population transport characteristics. We, therefore, used extracellular ADIFAB, where its calibration has been confirmed extensively (15), to monitor the time course of FFA uptake by suspensions of cardiomyocytes. The change in ADIFAB fluorescence was used to determine the decrease in FFA_o and, therefore, the uptake of FFA from extracellular FFA-BSA complexes to the cardiomyocytes (Fig. 3). In this representative experiment, the addition of $\sim 5 \times 10^4$ cardiomyocytes to a cuvette containing ADIFAB and a weakly (BSA = 10 μM) buffered OA-BSA complex resulted in a decrease in OA_o from 150 to ~92 nM during the 1000-s period of this measurement. The time course for the OA transfer was well described by two components, a single exponential decay yielding a rate constant of 0.011 ± 0.0004 s^{-1} and an approximately linear decay yielding a slope of 0.020 ± 0.001 nM/s (Fig. 3*A*).

The rate constant for the initial portion of the time course of uptake (0.011 s^{-1}) is virtually the same as the values of ~0.01 s^{-1} obtained from the intracellular ADIFAB and BCECF-AM experiments. The initial portion of the uptake time course, therefore, likely reflects FFA influx (k_{in}). The equivalence of rate constants determined from intracellular and extracellular measurements further supports intracellular ADIFAB as a reliable indicator of FFA kinetics.

We suggest that the slower portion of the time course reflects metabolism of FFA. Treating cells with the CPT-1 inhibitor etomoxir resulted in a 5-fold reduction in the slope of linear component of transfer, consistent with this component representing FFA metabolism (Fig. 3, *B* and *C*). Moreover, the rate constants and amplitudes of the fast component of uptake (influx) were virtually identical in etomoxir-treated and control cells. In addition, etomoxir had no effect on OA_i as measured in cells microinjected with ADIFAB (Fig. 3*D*). These results indicate that rate constant for FFA translocation and the initial flux of FFA across the plasma membrane are decoupled from FFA metabolism.

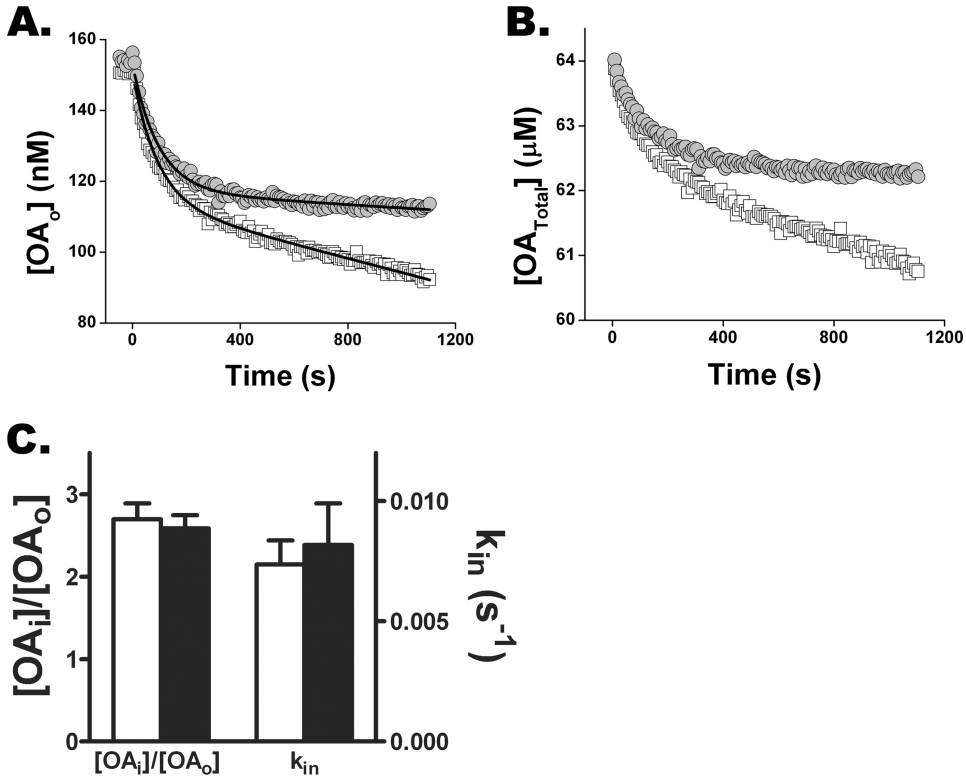

FIGURE 3. **Monitoring FFA uptake differentiates transport from metabolism in cardiomyocytes.** Cardiomyocytes (4.2×10^4) were added to a stirred cuvette containing a weakly buffered OA-BSA complex (BSA = 10 μM) and 0.2 μM ADIFAB. The ratio of 505 and 432-nm fluorescence intensities was measured every 8 s, from which OA_o values were computed as described (15). *A*, comparison of oleate uptake by cardiomyocytes untreated (*open boxes*) and treated (*filled circles*) with 10 μM etomoxir for 15 min is shown. For the first component of uptake, the rate constants 0.011 and 0.010 s^{-1} and the decrease in OA_o, 33.1 and 32.9 nM, were virtually identical for control and etomoxir treated cardiomyocytes. In contrast, the slope of the linear component decreased 5-fold, from 0.02 to 0.004 nM/s for etomoxir-treated cells. *B*, uptake data of *A*, represented as $[OA_{Total}]$, was calculated using Equation 2. *C*, etomoxir treatment (*filled bars*) of microinjected cardiomyocytes does not affect OA_i or k_{in} for well buffered OA_o (600 μM BSA). Results are from four etomoxir-treated and untreated cells.

Cardiomyocytes Concentrate FFA—We observed $FFA_i > FFA_o$ gradients in adipocytes and preadipocytes and found that metabolic inhibition reduced the gradients (11, 12). Treatment of cardiomyocytes with the ATP reducing agents oligomycin and 2-deoxyglucose also resulted in reduced gradients (Fig. 4*A*). Gradients were not completely abolished, but increasing the duration of treatment for more than 30 min, which we found was required for complete ATP depletion of adipocytes and preadipocytes (12), resulted in predominantly nonviable cardiomyocytes. We investigated whether the $FFA_i > FFA_o$ gradient in cardiomyocytes was a function of FFA_o or total extracellular FFA by measuring transport with OA-BSA complexes for which BSA was 300, 600, or 900 μM. For each complex the corresponding total OA was adjusted so that OA_o was fixed at 50 nM. Essentially the same k_{in} (data not shown) and the same OA_i (150 nM) at steady state was observed for all three complexes, demonstrating that the initial FFA influx rate and the $OA_i > OA_o$ gradient are functions of FFA_o rather than extracellular total FFA (Fig. 4, *B* and *C*). In these experiments (Fig. 4*B*) the total OA concentration was increased 3-fold to maintain a constant OA:BSA ratio, and as a consequence the total FFA gradient also increased 3-fold (Fig. 4*D*) without, however, altering the FFA influx rate or the FFA_u gradient.

FFA Transport Is Saturable—The ability to generate a concentration gradient suggests that transport may be mediated by a specific membrane protein and should, therefore, be saturable with increasing FFA_o. Measurements of OA transport, in fact, revealed that the initial rate of influx (nM/s) saturated and the FFA_i/FFA_o gradient decreased with increasing OA_o (Fig. 5). These transport kinetics were well described by a carrier model described previously (11, 24), which yielded a maximum influx velocity (R_{max}) of ~6 nM/s, and dissociation constant (K_o) for binding to the extracellular face of the carrier of ~100 nM.

Influx and Efflux Rate Constants Decrease with Increasing FFA_o—The formation of an $FFA_i > FFA_o$ concentration gradient appears inconsistent with faster efflux than influx (Table 1). Similar considerations for adipocytes led to the finding that efflux rate constants decreased with increasing FFA_o and suggested that efflux might be regulated by an FFA_o sensing gate (11). We investigated the FFA_o dependence of efflux in cardiomyocytes by stimulating influx with OA_o ~ 150 nM and, after reaching steady state, efflux was initiated by clamping OA_o at levels between 0 and 20 nM. We observed that k_{out} decreased by more than 4-fold over this OA_o range (Fig. 6*A*). In addition, we found that k_{in} decreased by ~2-fold for OA_o between 20 and 100 nM (Fig. 6*B*). Because efflux decreases more rapidly than influx, k_{out} becomes slower than k_{in} at $FFA_o > 0$, thereby allowing the formation of a gradient.

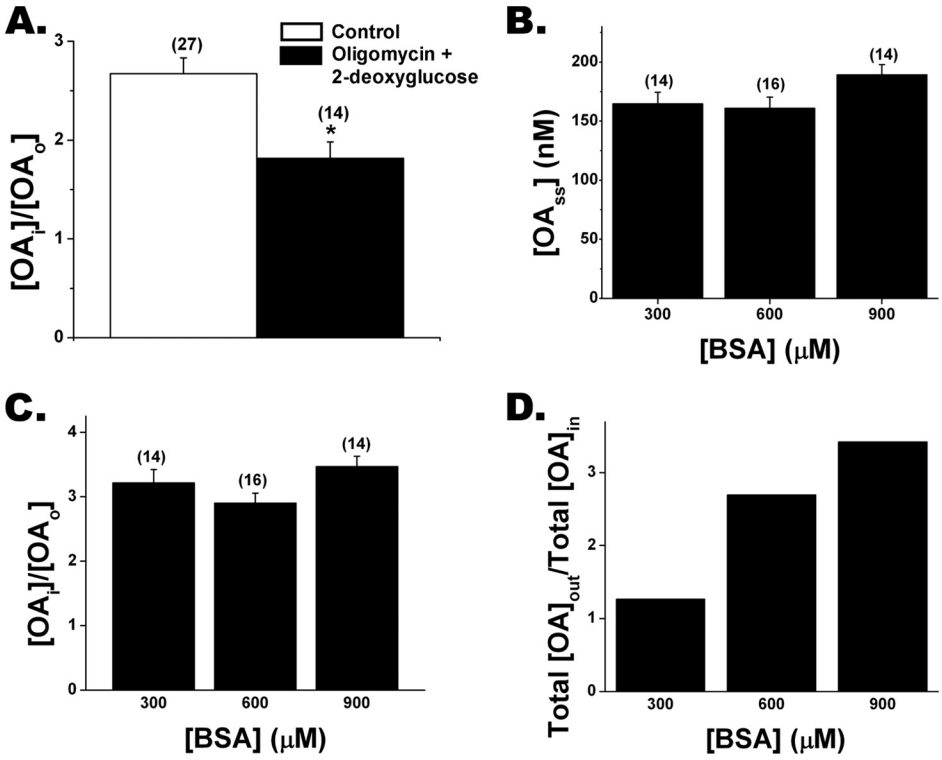

FIGURE 4. **Oligomycin plus 2-deoxyglucose treatment decreases FFA_i/FFA_o.** *A*, treatment of cardiomyocytes with 10 μg/ml oligomycin and 37 mM 2-deoxyglucose for 30 min reduced the gradient in cardiomyocytes. *B*, steady state FFA_i is independent of total extracellular FFA as demonstrated using OA-BSA complexes of 300, 600, and 900 μM BSA with total FFA adjusted so that $OA_o \sim 50$ nM for each complex. The number of cells investigated in each case is shown in *parentheses*. Results from *B* were used to determine the FFA_u gradient (*C*) and total FFA gradient (*D*) as a function of BSA concentration. *D*, total FFA gradients were calculated using Equation 3 and data from *B*.

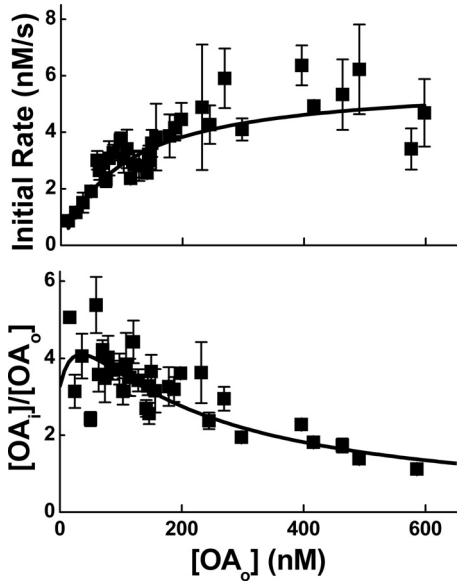

FIGURE 5. **FFA transport reveals saturation with increasing FFA_o.** *Upper panel*, the initial rate of influx as a function of increasing OA_o is shown. *Lower panel*, shown is the concentration gradient OA_i/OA_o, also as a function of increasing OA_o. Results for *both panels* were obtained from 154 transport cycles using cells derived from hearts isolated from 14 C57BL/6 mice. Five transport cycles were used per data point. Results of *both panels* were well described ($R^2 = 0.85$) by a carrier model (*solid lines*) with maximum velocity $R_{max} \sim 6$ nM/s and a dissociation constant for binding to the extracellular face of the carrier $K_o \sim 100$ nM.

$FAT/CD36^{-/-}$ Cardiomyocytes Reveal Slower FFA Efflux than WT Cells—Our results for WT cardiomyocytes are consistent with a membrane protein-mediated transport mechanism. Previous studies have reported that FFA uptake in cardiomyocytes is mediated at least in part by FAT/CD36 (3, 9). Using ADIFAB microinjected cardiomyocytes isolated from $FAT/CD36^{-/-}$ mice, we found that OA transport was consistent with a saturable mechanism revealing $FFA_i > FFA_o$ gradients similar to WT cells (Fig. 7, *A* and *B*). Influx was not significantly reduced in $FAT/CD36^{-/-}$ cells except for $OA_o = 20$ nM, where k_{in} was ~50% slower than for WT cells (Fig. 7*C*). In contrast, k_{out} was significantly slower in $FAT/CD36^{-/-}$ as compared with WT cells for all OA_o measured, leading to a 2–3-fold reduction in the initial rate of efflux (Fig. 7*D*). These results indicate that the transport/pumping mechanism is largely intact in $FAT/CD36^{-/-}$ cells but raise the possibility that CD36 interacts with the transporter to modulate FFA efflux and influx rate constants.

DISCUSSION

We have used quantitative imaging of FFA_i to determine the rate constants for FFA influx and efflux as well as the steady state FFA_i levels in isolated cardiomyocytes. The measurements are consistent with FFA transport mediated by a saturable pump whose efflux and influx rates are modulated by interaction with FAT/CD36. These results, obtained using microinjected ADIFAB, were confirmed by monitoring pH_i using BCECF-AM and by measurements of FFA uptake monitored using extracellular ADIFAB. The results also indicate that the rate constant and initial rate of FFA transport across the plasma membrane of cardio-

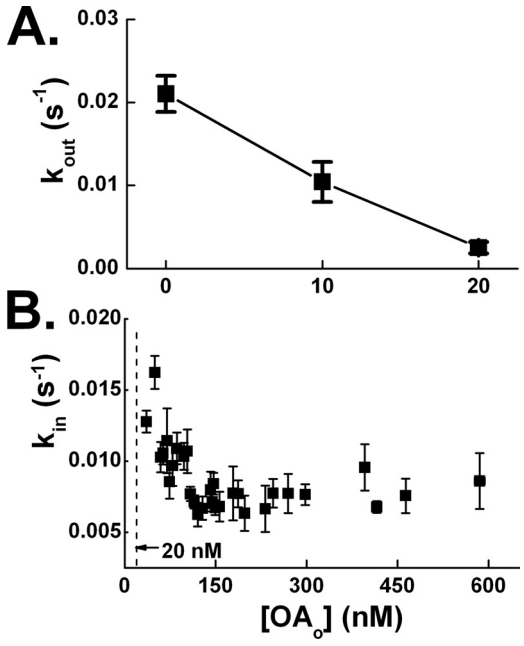

FIGURE 6. **Efflux and influx rate constants decrease with increasing FFA_o in cardiomyocytes.** *A*, efflux rate constants were measured after initiating influx by exposing cardiomyocytes to OA_o = 150 nM. Cells were allowed to reach steady state, at which time OA_i was ~500 nM. At that point the extracellular buffer containing OA_o = 150 nM was exchanged for a buffer in which OA_o was clamped at concentrations of 0, 10, and 20 nM, and k_{out} was determined. Data were obtained from three cells exposed to the same complexes. *B*, influx rate constants (k_{in}) were determined for increasing OA_o. Data were obtained from 154 transport cycles derived from cardiomyocytes isolated from the hearts of 14 mice. An average of five transport cycles per data point is shown.

myocytes is highly regulated and is unaffected by inhibition of fatty acid oxidation.

Previous studies have reported evidence for both protein (29–32)- and non-protein (33, 34)-mediated transport in cardiomyocytes. With the exception of Wu *et al.* (34), these studies involved measurements of uptake of radioactively labeled FFA (29–33). For uptake to accurately reflect FFA transport, it is essential that transport be stopped after the cells are washed with albumin to remove extracellular FFA in the medium. However, washing can remove virtually all (>98%) FFA transported into cells (11, 12, 24) as is also evident from Figs. 1 and 2, which reveal that FFA are extracted from the cardiomyocytes within 100 s after adding albumin. In addition, as we discussed previously in Kampf *et al.* (12), determining that transport is saturable with increasing FFA_o depends critically on the accuracy of FFA_o at large values where buffering by FFA-BSA complexes may fail. In previous studies (6, 30, 35, 36) FFA_o were calculated using published FFA-BSA binding affinities, and these calculated values were likely larger than the actual FFA_o, thereby possibly giving the appearance of saturation. This is demonstrated in Fig. 3, where FFA_o decreased significantly under weak, low BSA, buffering conditions. To avoid these complications and to directly monitor FFA_i and FFA_o levels, our studies used methods that allowed continuous monitoring of FFA transport without the need for removing extracellular FFA. This method also allowed direct measurement of FFA_o under both well buffered and weakly buffered conditions.

Wu *et al.* (34) used BCECF-AM-loaded cardiomyocytes to monitor FFA-mediated pH_i changes and observed slower influx ($t_{½} > 300$ s) but similar efflux times ($t_{½} < 30$ s) as in the present study. The lack of transport saturation observed by Wu *et al.*, (34) we suggest likely resulted from using uncomplexed FFA and not measuring FFA_o. Although Wu *et al.* (34) concluded that transport was mediated by a lipid phase mechanism, lipid phase transport is >100-fold faster than in cardiomyocytes (28). Moreover, dissociation is the rate-limiting step in the proposed (34) lipid mechanism, whereas the virtually identical influx rate constants from ADIFAB (depends on translocation and dissociation) and BCECF-AM (depends on translocation only) measurements demonstrate (11) that translocation, not dissociation, is rate-limiting for cardiomyocytes. Flip-flop is also the rate-limiting step for FFA transport across lipid vesicles but, as indicated above, is much faster than in cardiomyocytes (28). Also, in contrast to lipid vesicles, where rate constants are highly sensitive to the FFA molecular species (18), we found that transport in cardiomyocytes reveals little or no dependence on FFA type (Table 1). These differences as well as transport saturability and FFA_u gradients, which are absent in lipid vesicles (37), indicate that FFA transport across cardiomyocytes is unlikely to be mediated by a lipid phase mechanism.

FFA Influx Is Mediated by an FFA Pump—Influx measurements in cardiomyocytes microinjected with ADIFAB reveal an $FFA_i > FFA_o$ gradient that is reduced by treatment with oligomycin plus 2-deoxyglucose (Fig. 4). Although ATP levels were not determined in these cells, oligomycin plus 2-deoxyglucose are known to reduce ATP levels (11, 19, 20), which suggests that an ATP-dependent pump may be the driving force for cellular uptake of FFA. This conclusion might be questioned because the FFA_i determination depends upon assumptions about the intracellular environment effect on intracellular ADIFAB. Such issues were addressed in detail in our studies of adipocyte transport (11), and we also obtained evidence for a gradient in adipocytes using imaging mass spectrometry (24). Nevertheless, we have in the present study obtained evidence for an $FFA_i > FFA_o$ gradient in cardiomyocytes that is independent of intracellular ADIFAB. To do this we assumed, as described in reference (24), that FFA_i and total FFA in the intracellular lipid phase are in equilibrium, which is governed by the lipid/water partition coefficient (K_p). For the uptake results of Fig. 3, we estimated that the total intracellular concentration of OA was 1.7 mM from the decrease in extracellular OA concentration (Fig. 3*C*) and the cellular volume of 30 pl for a cardiac myocyte (38). These values together with the previously measured K_p for OA (4×10^5 (15)), a cellular lipid concentration of 23 mM (23), and Equation 3, predict OA_i = 231 nM. FFA_o at steady state (~250 s in Fig. 3*A*) was 118 nM, and therefore, OA_i was twice OA_o for the experiment of Fig. 3. Thus, uptake measurements are also consistent with an $FFA_i > FFA_o$ gradient.

These results would seem to conflict with metabolism being the driving force for transporting FFA from blood into cardiomyocytes, which would be expected to result in intracellular total FFA < extracellular total FFA. Studies in cardiac and skeletal muscle have indicated a total FFA concentration

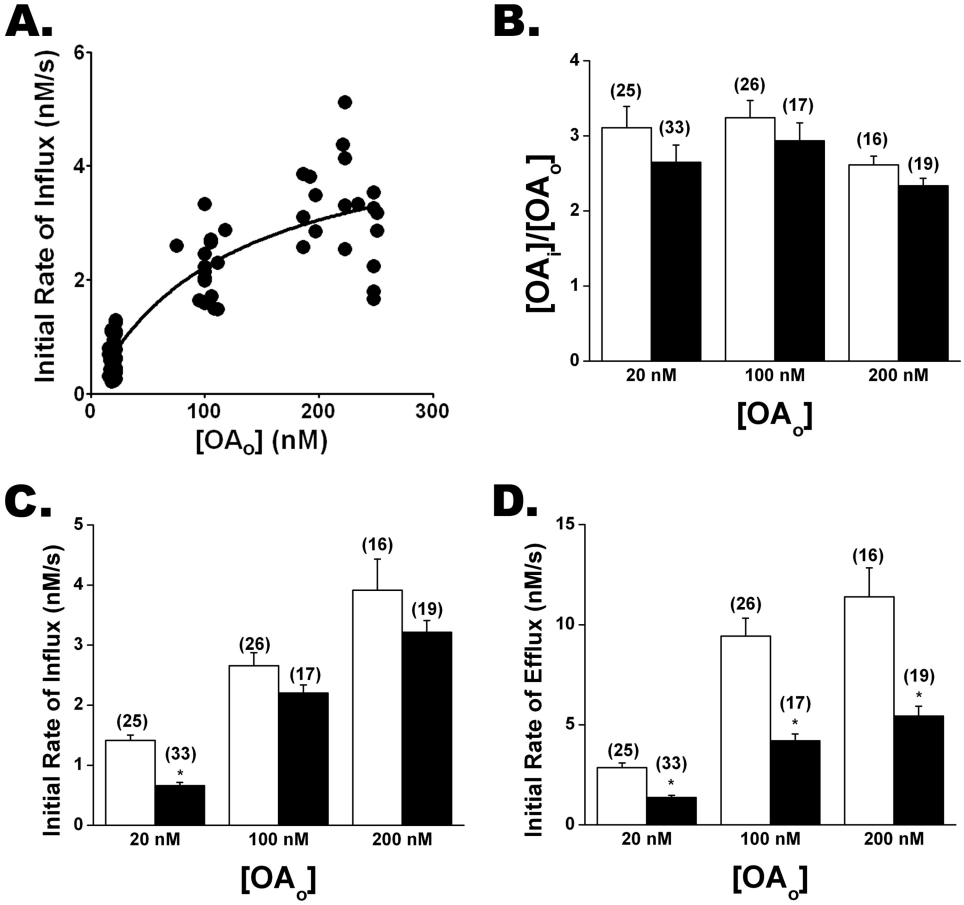

FIGURE 7. **Oleate transport in FAT/CD36$^{-/-}$ and WT cardiomyocytes.** *A*, initial rates of influx *versus* the OA$_o$ for FAT/CD36$^{-/-}$ cardiomyocytes were well described by the carrier model ($R^2 = 0.78$) with $R_{max} \sim 5$ nM/s and $K_o \sim 120$ nM. The data were significantly nonlinear ($p = 0.045$). *B*, OA$_i$/OA$_o$ gradients for WT (*white*) and FAT/CD36$^{-/-}$ (*black*) cardiomyocytes for increasing OA$_o$ are shown. *C*, initial rates of influx are shown. *D*, initial rates of efflux are shown. Averages of *N* transport cycles are indicated in *parentheses*.

in blood that was 3–12-fold larger than in cardiac tissue (39, 40), suggesting that the driving force for FFA uptake was a low tissue FFA maintained by FFA metabolism. For the measurements of Fig. 3, the ratio of extracellular (62.6 μM) to cellular (1.7 mM) total OA was ~0.04 at the end of the first component of transfer, the opposite of what has been observed in cardiac and skeletal muscle (39). However, BSA was 10 μM in the Fig. 3 study. For physiologic BSA (600 μM), the ratio of extracellular (3.8 mM, corresponding to OA$_o$ = 118 nM) to cellular (1.7 mM) total OA would be ~2.2, consistent with *in vivo* results (39). These observations and those of Fig. 4 indicate that the driving force for FFA transport is the unbound rather than total FFA gradient.

To summarize, our results indicate that FFAs are rapidly transported up a FFA$_u$ concentration gradient, and under physiologic conditions, where FFA$_o$ is well buffered, FFA$_i$ is maintained at a level that is 3–10-fold larger than FFA$_o$. Under these conditions the high FFA$_i$ levels provide a constant reservoir of FFA so that FFA$_i$ are not rate-limiting for the relatively slow rate of FFA metabolism. For these well-buffered conditions, at steady state both FFA$_o$ and FFA$_i$ are unchanging, whereas FFA metabolism mediates a net FFA flux into the cells. We estimated the initial flux of total FFA using the data of Fig. 5, *upper panel*, Equation 3, and a cardiomyocyte volume of 30 pl. This estimate yielded an initial flux that ranges from 1 to 5 $\times$ 10^8 molecules of FFA/cell/s.

Cardiomyocyte FFA Transporter Characteristics May Be Modulated by FAT/CD36—Transport characteristics of cardiomyocytes revealed by the present studies are similar to but not identical to those we reported previously for adipocytes and preadipocytes (11, 12). Influx and efflux rate constants are about 2–3-fold slower and the FFA$_i$>FFA$_o$ gradients at least 50% larger in cardiac myocytes than in adipocytes and preadipocytes. Transport in both types of cells is consistent with a carrier model, albeit with differences in parameters that reflect the observed differences in transport characteristics. The maximum influx rate (6 nM/s) and dissociation constant (100 nM) are about 50% smaller for the cardiac myocytes (Fig. 5) than adipocytes. Although normal circulating FFA$_o$ are generally less than 3 nM (41, 42), cardiac specific lipoprotein lipase activity may increase FFA$_o$ in the region immediately adjacent to the cardiomyocyte. Goldberg and co-workers (43) have demonstrated that lipoprotein lipase activity is important for providing myocardial FFA. Albumin-bound FFA may be insufficient possibly because circulating FFA$_o$ are low and higher local FFA$_o$ are required for efficient myocardial function. Therefore, a $K_o \sim 100$ nM may be appropriate for myocardial transport. This is similar to the mechanism we postu-

lated for adipocytes under postprandial conditions where adipocyte lipoprotein lipase activity presumably increases FFA_o levels to match the $K_o \sim 150$ nM of the adipocyte (11).

A similar protein may, therefore, be responsible for FFA transport in adipocytes, cardiomyocytes, and preadipocytes. Among the proteins reported to contribute to FFA uptake, FAT/CD36 has been associated with uptake in both adipocytes and cardiomyocytes (9, 44, 45). However, we found virtually identical transport characteristics in adipocytes, which express FAT/CD36, and preadipocytes, in which expression of FAT/CD36 is <5% that of adipocytes (12, 13). Moreover, FFA transport characteristics we observed in cardiomyocytes obtained from FAT/CD36$^{-/-}$ mice are largely similar to those from WT mice (Fig. 7). Nevertheless, because in FAT/CD36$^{-/-}$ mice efflux rates were reduced and influx was reduced when $FFA_o = 20$ nM, our results suggest that FAT/CD36 may interact with the transporter. This reduction in influx rates at low FFA_o is consistent with previous results examining the role of FAT/CD36 in cardiac FFA transport for which FFA_o was generally <20 nM (6). A possible mechanism for modulation of transport by FAT/CD36 that would lead to slower efflux in FAT/CD36$^{-/-}$ cells is through the gating mechanism (Fig. 6). If FAT/CD36 were involved in maintaining the gate in an open state at zero FFA_o, then the absence of FAT/CD36 expression would lead to slower efflux rates as depicted in Fig. 7. Because no significant differences in transport characteristics were observed between adipocytes and preadipocytes, we suggest that the transporter-FAT/CD36 interaction is specific for cardiomyocytes.

Acknowledgment—We greatly appreciate the gift of the FAT/CD36$^{-/-}$ mice from Dr. Nada Abumrad (Washington University in St. Louis).

REFERENCES

1. Szczepaniak, L. S., Victor, R. G., Orci, L., and Unger, R. H. (2007) *Circ. Res.* **101,** 759–767
2. Kampf, J. P., and Kleinfeld, A. M. (2007) *Physiology* **22,** 7–14
3. Bonen, A., Chabowski, A., Luiken, J. J., and Glatz, J. F. (2007) *Physiology* **22,** 15–29
4. Hamilton, J. A. (2007) *Prostaglandins Leukot. Essent. Fatty Acids* **77,** 355–361
5. Ibrahimi, A., and Abumrad, N. A. (2002) *Curr. Opin. Clin. Nutr. Metab Care* **5,** 139–145
6. Luiken, J. J., Turcotte, L. P., and Bonen, A. (1999) *J. Lipid Res.* **40,** 1007–1016
7. Turcotte, L. P., Swenberger, J. R., Tucker, M. Z., Yee, A. J., Trump, G., Luiken, J. J., and Bonen, A. (2000) *Mol. Cell. Biochem.* **210,** 53–63
8. Koonen, D. P., Glatz, J. F., Bonen, A., and Luiken, J. J. (2005) *Biochim. Biophys. Acta* **1736,** 163–180
9. Brinkmann, J. F., Abumrad, N. A., Ibrahimi, A., van der Vusse, G. J., and Glatz, J. F. (2002) *Biochem. J.* **367,** 561–570
10. Nickerson, J. G., Alkhateeb, H., Benton, C. R., Lally, J., Nickerson, J., Han, X. X., Wilson, M. H., Jain, S. S., Snook, L. A., Glatz, J. F., Chabowski, A., Luiken, J. J., and Bonen, A. (2009) *J. Biol. Chem.* **284,** 16522–16530
11. Kampf, J. P., and Kleinfeld, A. M. (2004) *J. Biol. Chem.* **279,** 35775–35780
12. Kampf, J. P., Parmley, D., and Kleinfeld, A. M. (2007) *Am. J. Physiol. Endocrinol. Metab.* **293,** E1207–E1214
13. Sandoval, A., Fraisl, P., Arias-Barrau, E., Dirusso, C. C., Singer, D., Sealls, W., and Black, P. N. (2008) *Arch. Biochem. Biophys.* **477,** 363–371
14. Richieri, G. V., Ogata, R. T., and Kleinfeld, A. M. (1992) *J. Biol. Chem.* **267,** 23495–23501
15. Richieri, G. V., Ogata, R. T., and Kleinfeld, A. M. (1999) *Mol. Cell. Biochem.* **192,** 87–94
16. Carley, A. N., Semeniuk, L. M., Shimoni, Y., Aasum, E., Larsen, T. S., Berger, J. P., and Severson, D. L. (2004) *Am. J. Physiol. Endocrinol. Metab* **286,** E449–E455
17. LoRusso, S. M., Imanaka-Yoshida, K., Shuman, H., Sanger, J. M., and Sanger, J. W. (1992) *Cell Motil. Cytoskeleton* **21,** 111–122
18. Kampf, J. P., Cupp, D., and Kleinfeld, A. M. (2006) *J. Biol. Chem.* **281,** 21566–21574
19. Seraydarian, M. W., Sato, E., Savageau, M., and Harary, I. (1969) *Biochim. Biophys. Acta* **180,** 264–270
20. Tatsumi, T., Shiraishi, J., Keira, N., Akashi, K., Mano, A., Yamanaka, S., Matoba, S., Fushiki, S., Fliss, H., and Nakagawa, M. (2003) *Cardiovasc. Res.* **59,** 428–440
21. Huber, A. H., Kampf, J. P., Kwan, T., Zhu, B., and Kleinfeld, A. M. (2006) *Biochemistry* **45,** 14263–14274
22. Demant, E. J., Richieri, G. V., and Kleinfeld, A. M. (2002) *Biochem. J.* **363,** 809–815
23. Forsdahl, K., and Larsen, T. S. (1995) *J. Mol. Cell. Cardiol.* **27,** 893–900
24. Kleinfeld, A. M., Kampf, J. P., and Lechene, C. (2004) *J. Am. Soc. Mass Spectrom.* **15,** 1572–1580
25. Greenwood, A. I., Tristram-Nagle, S., and Nagle, J. F. (2006) *Chem. Phys. Lipids* **143,** 1–10
26. Anel, A., Richieri, G. V., and Kleinfeld, A. M. (1993) *Biochemistry* **32,** 530–536
27. Caserta, F., Tchkonia, T., Civelek, V. N., Prentki, M., Brown, N. F., McGarry, J. D., Forse, R. A., Corkey, B. E., Hamilton, J. A., and Kirkland, J. L. (2001) *Am. J. Physiol. Endocrinol. Metab.* **280,** E238–E247
28. Carley, A. N., and Kleinfeld, A. M. (2009) *Biochemistry* **48,** 10437–10445
29. Febbraio, M., Abumrad, N. A., Hajjar, D. P., Sharma, K., Cheng, W., Pearce, S. F., and Silverstein, R. L. (1999) *J. Biol. Chem.* **274,** 19055–19062
30. Stremmel, W. (1988) *J. Clin. Invest.* **81,** 844–852
31. Sorrentino, D., Stump, D., Potter, B. J., Robinson, R. B., White, R., Kiang, C. L., and Berk, P. D. (1988) *J. Clin. Invest.* **82,** 928–935
32. Luiken, J. J., van Nieuwenhoven, F. A., America, G., van der Vusse, G. J., and Glatz, J. F. (1997) *J. Lipid Res.* **38,** 745–758
33. DeGrella, R. F., and Light, R. J. (1980) *J. Biol. Chem.* **255,** 9731–9738
34. Wu, M. L., Chan, C. C., and Su, M. J. (2000) *Circ. Res.* **86,** E55–E62
35. Bastie, C. C., Hajri, T., Drover, V. A., Grimaldi, P. A., and Abumrad, N. A. (2004) *Diabetes* **53,** 2209–2216
36. Sorrentino, D., Robinson, R. B., Kiang, C. L., and Berk, P. D. (1989) *J. Clin. Invest.* **84,** 1325–1333
37. Cupp, D., Kampf, J. P., and Kleinfeld, A. M. (2004) *Biochemistry* **43,** 4473–4481
38. Satoh, H., Delbridge, L. M., Blatter, L. A., and Bers, D. M. (1996) *Biophys. J* **70,** 1494–1504
39. Van der Vusse, G. J., Roemen, T. H., Flameng, W., and Reneman, R. S. (1983) *Biochim. Biophys. Acta* **752,** 361–370
40. Van der Vusse, G. J., and Roemen, T. H. (1995) *J. Appl. Physiol.* **78,** 1839–1843
41. Cantor, W. J., Kim, H. H., Jolly, S., Moe, G., Burstein, J. M., Mendelsohn, A., Kleinfeld, A. M., and Fitchett, D. (2008) *J. Invasive Cardiol.* **20,** 186–188
42. Apple, F. S., Kleinfeld, A. M., and Adams, J. E. (2004) *Clin. Proteomics* **1,** 41–44
43. Augustus, A. S., Buchanan, J., Park, T. S., Hirata, K., Noh, H. L., Sun, J., Homma, S., D'armiento, J., Abel, E. D., and Goldberg, I. J. (2006) *J. Biol. Chem.* **281,** 8716–8723
44. Luiken, J. J., Willems, J., van der Vusse, G. J., and Glatz, J. F. (2001) *Am. J. Physiol. Endocrinol. Metab.* **281,** E704–E712
45. Coburn, C. T., Knapp, F. F., Jr., Febbraio, M., Beets, A. L., Silverstein, R. L., and Abumrad, N. A. (2000) *J. Biol. Chem.* **275,** 32523–32529